Progress In Electromagnetics Research M, Vol. 70, 51–60, 2018

Slotted Folded Substrate Integrated Waveguide Band Pass Filter with Enhanced Bandwidth for Ku/K Band Applications

Nitin Muchhal[1, *], Arnab Chakraborty[1], Manoj Vishwakarma[2], and Shweta Srivastava[1]

Abstract—This paper proposes the design of wide bandpass filters for Ku and Ku/K band applications. It has wide passband with miniaturization of size using folded substrate integrated waveguide (FSIW) technique. The filter is designed by introducing a C slot and an E slot in central metallic septum of FSIW respectively. The proposed filters are simulated, fabricated after optimization and finally tested. The fabricated E slot filter achieved enhancement in bandwidth with dual-band operating in Ku band (14.35 GHz–16.76 GHz) and K band (18.66 GHz–19.61 GHz), respectively. The measured results match quite closely with simulated ones.

1. INTRODUCTION

In recent times, there has been an emergent emphasis on the development of miniaturized, wide-band and advanced microwave and millimetre wave systems. To achieve this demand, communication systems are expeditiously shifting to higher frequency ranges, and there have been tremendous growth, demand and immense prospects in microwave bands especially X, Ku and K bands. This growth is the consequence of tremendous demand in the area of satellite communication (SATCOM) [1] for the applications in the area of internet access [2] to remote areas, defence, entertainment, satellite phones, satellite television, etc. Ku and K band's microwave domain is primarily utilized for satellite and radar applications. The conventional rectangular waveguide (RWG) has benefits of possessing high Q and low loss. However, it is difficult to fabricate, expensive for mass production and tedious to integrate with planar circuits. Also, higher frequencies prevent the application of planar technology due to high transmission losses. The prospective solution for overcoming this problem at higher frequency is substrate-integrated waveguide (SIW) technology [3]. SIW technology is becoming the future technology for planar transmission line as it has the benefit of easy integration and compact size in comparison to traditional microstrip structures [4].

There are various methods used to increase the bandwidth of a substrate integrated waveguide bandpass filter. Chen et al. [5] proposed a multiple-mode resonator (MMR) to realize a wide passband operation. They accomplished it by etching the upper layer of an SIW cavity embedded with U-shape slots. Dong et al. [6] designed a wideband bandpass filter by etching dumbbell slots on the bottom and top metallic planes of an SIW cavity. Hosseini-Fahraji et al. [7] proposed a wideband bandpass filter for millimetre-wave by cutting rectangular shape slots on the upper metallic plane of an SIW cavity and achieved wide bandpass response. Recently Liu and An [8] proposed a bandpass filter by integrating modified dumbbell defected ground structure (DGS) cells with SIW and achieved wide band of operation. In the same year, Wu et al. [9] proposed and designed a compact wideband quarter mode SIW bandpass filter by etching a meandered H-shaped slot on the cavity and demonstrated the effect of slot length and its position on the bandwidth.

Received 18 April 2018, Accepted 21 June 2018, Scheduled 3 July 2018
* Corresponding author: Nitin Muchhal (nmuchhal@gmail.com).
[1] Department of Electronics and Communication, Jaypee Institute of Information Technology, Noida, India. [2] Department of Electronics and Communication, IEC College of Engineering & Technology, G. Noida, India.

The present paper proposes the design of two wide bandpass filters using Folded SIW (FSIW) technique for Ku/K band. A C-shaped slot and an E-shaped slot are etched on the central septum to obtain single band and dual band responses, respectively. The proposed bandpass filters using slots are analyzed using EM simulator software (Ansoft HFSS). To validate the analysis and design, the filter prototypes are fabricated, and the measured results validate the optimum performance of the proposed filters.

2. THE FSIW STRUCTURE

It has been established [10] that the FSIW has almost same propagation characteristics and cutoff frequency as possessed by SIW provided that the width of the FSIW is nearly half of the width of the original SIW and that its height is twice that of the SIW as shown in Fig. 1. That the horizontal section of FSIW is reduced to half results in size miniaturization. Based on transmission line theory and analytical Method of Moments (MoM) and cutoff frequency of the fundamental mode TE_{10} of FSIW, its width and gap are given by [10].

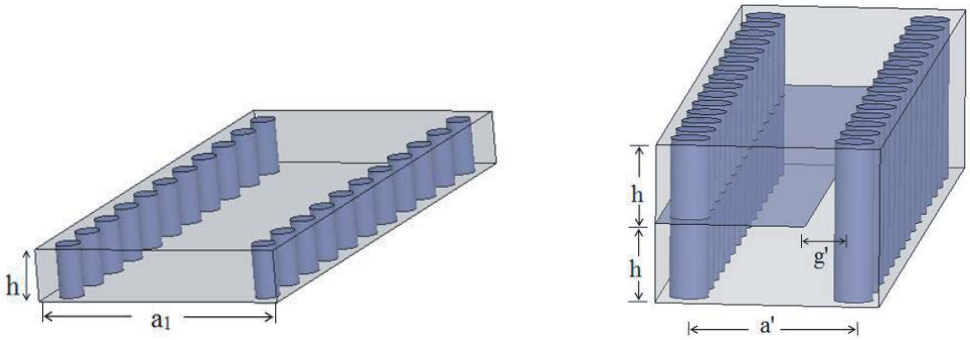

Figure 1. Configurations of SIW and FSIW.

The propagation constant for a folded SIW (FSIW) is given by

$$\beta\text{FSIW} = \sqrt{k^2 - \left[\frac{2}{a}\cot^{-1}\left(\frac{\mu a h \omega^2}{2\pi}C\right)\right]^2} \tag{1}$$

$$\pi f_c\sqrt{\mu\varepsilon} = \frac{1}{a}\text{arc}\cot\left(4f_c h\sqrt{\mu\varepsilon}\ln\left[\frac{h}{c_f}\left(\frac{1}{g}-\frac{2}{a}\right)\right]\right) \tag{2}$$

where $C = \frac{4\varepsilon}{\pi}\ln\left[\frac{h\left(1-\frac{2g}{a}\right)}{c_f g}\right]$.

Also the width and gap of FSIW are found from:

$$a' = \frac{a_1}{2} + \frac{a_1 - a}{2} = a_1 - \frac{a}{2} \tag{3}$$

$$g' = \frac{ah}{2h + c_f a e^{\frac{a_1^2}{2ah}\cot\left(\frac{\pi a}{2a_1}\right)}} + \frac{a_1 - a}{2} \tag{4}$$

where 'a_1' is the width of SIW, while 'a' is the width of its equivalent RWG.

2.1. Analysis and Design of Folded Substrate Integrated Waveguide (FSIW)

SIW has several benefits such as light weight, low leakage losses, and good invulnerability to electromagnetic interference. However, compared with stripline or microstrip components, SIW has a disadvantage of larger width for same circuits. To overcome this problem, the conception of Folded Substrate Integrated Waveguides (SIFW) was introduced by [11]. To miniaturize the SIW components,

various techniques have been reviewed by [12]. The design equations [13] for a substrate integrated waveguide (SIW) are:

Equivalent width of dielectric filled rectangular waveguide

$$W_{EQ} = \frac{c}{2f_c\sqrt{\varepsilon_r}} \tag{5}$$

Width of SIW,

$$W_{\text{SIW}} = W_{EQ} + \frac{D^2}{0.95P} \tag{6}$$

In addition for selecting P and D, following inequalities should be satisfied

$$P < 4D \quad \text{and} \quad P < \frac{\lambda_O}{2}\sqrt{\varepsilon_r} \tag{7}$$

For design of an SIW with cutoff frequency, $f_c = 14\,\text{GHz}$, dielectric constant, $\varepsilon_r = 2.5$, and height of SIW, $H = 1.6\,\text{mm}$, the design parameters are found as: $P = 1.2\,\text{mm}$, $D = 0.80\,\text{mm}$ and $W_{\text{SIW}} = 7.20\,\text{mm}$. Figs. 2(a) and 2(b) show the top and side views of a (C type) folded SIW with transition. Here W_{FSIW} is the width of folded SIW which is reduced to half of conventional SIW, L_{FSIW} the length of FSIW, and G the gap between the right sidewall and middle conductive septum. Therefore, design parameters of folded SIW are: $W_{\text{FSIW}} = 3.60\,\text{mm}$, $H_{\text{FSIW}} = 3.2\,\text{mm}$, $G = 1.1\,\text{mm}$, $L_{\text{FSIW}} = 19\,\text{mm}$, length of rectangular transition $L_T = 4\,\text{mm}$, width of transition $W_T = 1.4\,\text{mm}$, pitch $P = 1.2\,\text{mm}$, and diameter of via, $D = 0.8\,\text{mm}$.

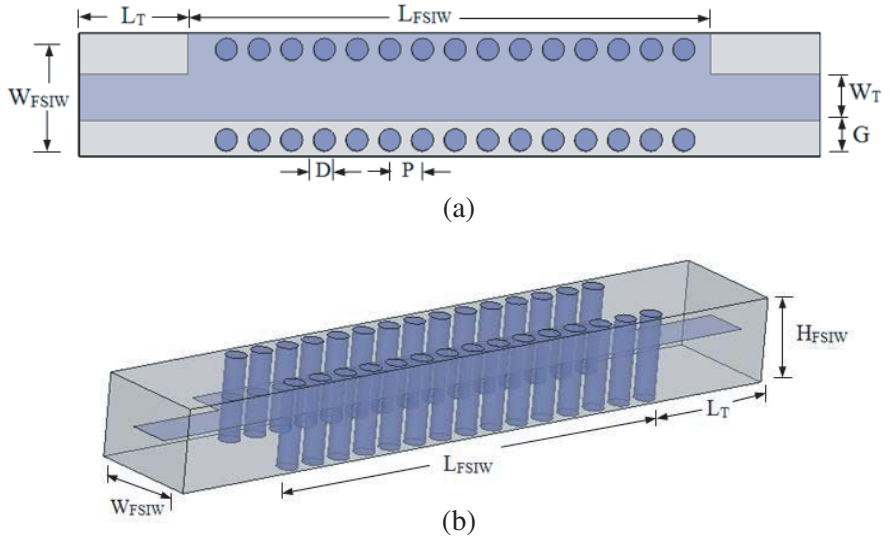

Figure 2. (a) Top view of FSIW with transition. (b) Side view of FSIW with transition.

Figure 3 compares the return loss and insertion loss curves of SIW and FSIW. From the figure it is evident that like SIW, FSIW has a similar high-pass performance with same cutoff frequency. The simulated result of FSIW as illustrated in Fig. 3 indicates that the reflection coefficient S_{11} remains well below $-10\,\text{dB}$, and the transmission coefficient S_{12} is around $-1.15\,\text{dB}$ across the entire pass band.

3. ANALYSIS AND DESIGN OF FSIW (WITH C SLOT ON CENTRAL METAL SEPTUM OF FSIW)

As shown in Fig. 4, a C slot is introduced on the central metal septum. Introducing a slot in the central conductor will change the electrical length of the folded SIW which will change the response of FSIW from High Pass to Band Pass. The geometry of modified FSIW is simulated using EM simulator HFSS

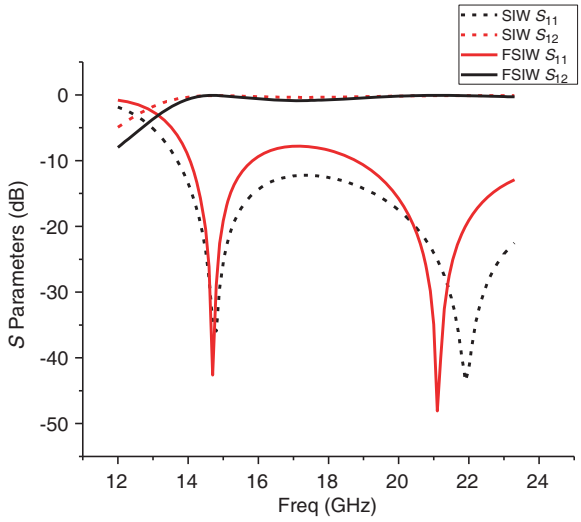

Figure 3. Comparison of S parameters of SIW and FSIW.

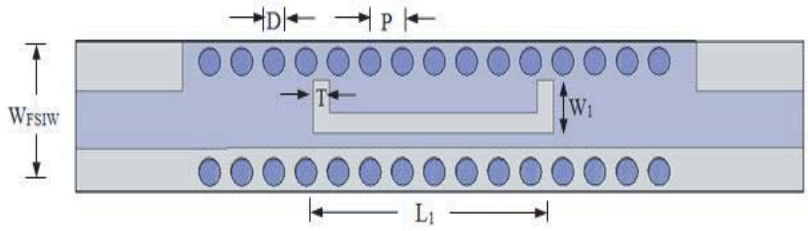

Figure 4. Folded SIW with C slot on central septum.

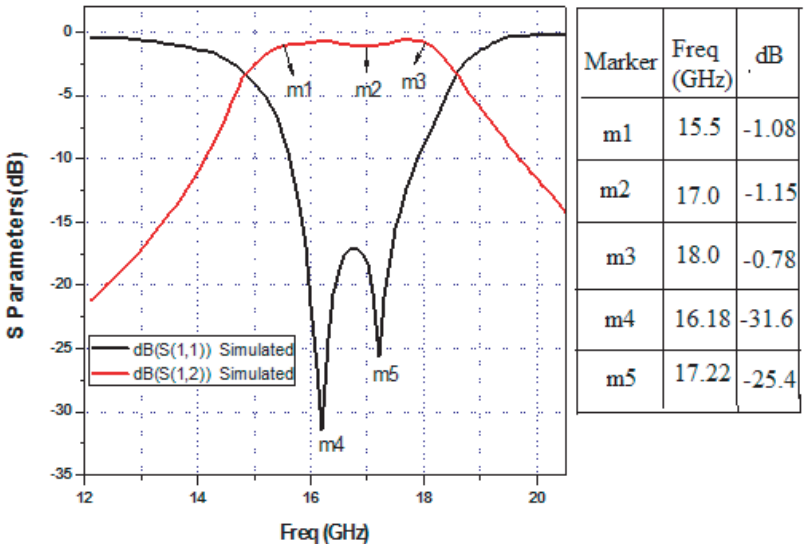

Figure 5. Simulated response of C slot FSIW.

v13 [14] by taking dielectric substrate glass PTFE having dielectric constant 2.5 and height 3.2 mm. The Loss tangent of the material is 0.002. The parameters of the C-slot as shown are given as follows: Length of slot $L_1 = 8$ mm, width of slot $W_1 = 2$ mm and thickness of slot $T = 0.65$ mm.

Figure 5 shows the simulated S parameter response of C slotted FSIW. From the frequency response, it is seen that the filter operates from 15.83 GHz to 18.12 GHz whose in-band insertion loss in passband is around −1.0 dB with maximum value as −1.15 dB, and in-band return loss is well below −17.5 dB with resonance peak at 16.18 GHz. From the graph, bandwidth at this resonance peak is 2.29 GHz with S_{11} peak at −31.65 dB. Fig. 6 shows the current distribution of C slot FSIW at the resonance peak. It is evident from current distribution that the current is concentrated on the side arms of the C slot. Fig. 7 shows the current distribution in stopband.

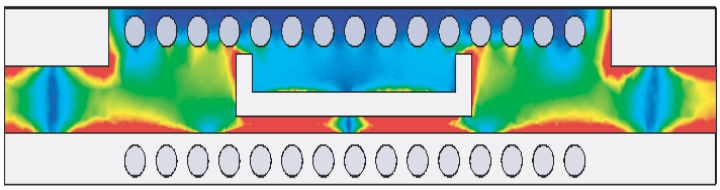

Figure 6. Current distribution of C slot FSIW at resonant freq. 16.18 GHz.

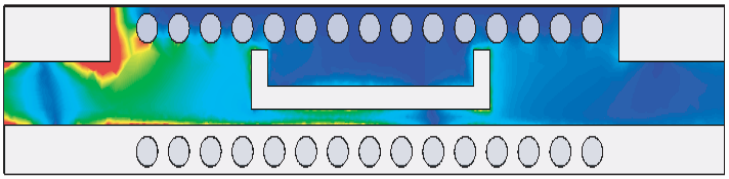

Figure 7. Current distribution of C slot FSIW in stop band.

4. ANALYSIS AND DESIGN OF FSIW (WITH E SLOT ON CENTRAL METAL SEPTUM OF FSIW)

In designing the second bandpass filter, an E slot is introduced on the central metal septum to change the response of FSIW from High Pass to Band Pass as shown in Fig. 8. The geometry of modified FSIW is simulated using EM simulator HFSS v13 [15] by taking dielectric substrate (glass PTFE) having dielectric constant 2.5 and height 3.2 mm. The loss tangent of the material is 0.002. The parameters of the E slot as shown in figure are given as follows: length of slot $L_2 = L_1 = 8$ mm, width of outer slot $W_2 = W_1 = 2$ mm, width of inner slot $W_2' = 1.35$ mm, and thickness of slot remains $T = 0.65$ mm.

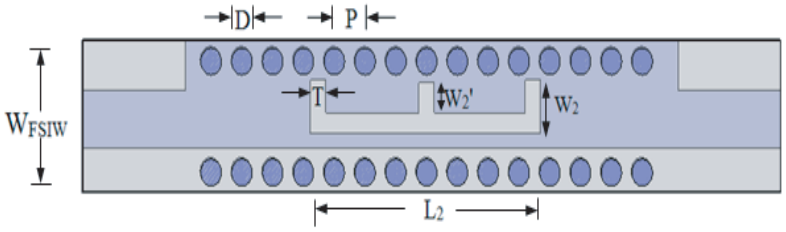

Figure 8. Folded SIW with C slot on central septum.

Figure 9 shows the simulated S parameter response of E slotted FSIW. From the frequency response, it is seen that the SIW dual-band filter operates in Ku band (14.15 GHz–16.66 GHz) and K band (18.64 GHz–19.7 GHz), whose in-band insertion losses are less than 1.50 dB with two resonance peaks at 14.7 GHz and 19.2 GHz, respectively. The maximum value of insertion loss in passband is −1.40 dB. From the graph, bandwidth at the first resonance peak is 2.51 GHz with S_{11} peak at 33.8 dB, and the bandwidth at the second resonance is 1.06 GHz with S_{11} peak at 26.4 dB. From Fig. 10, it is evident that

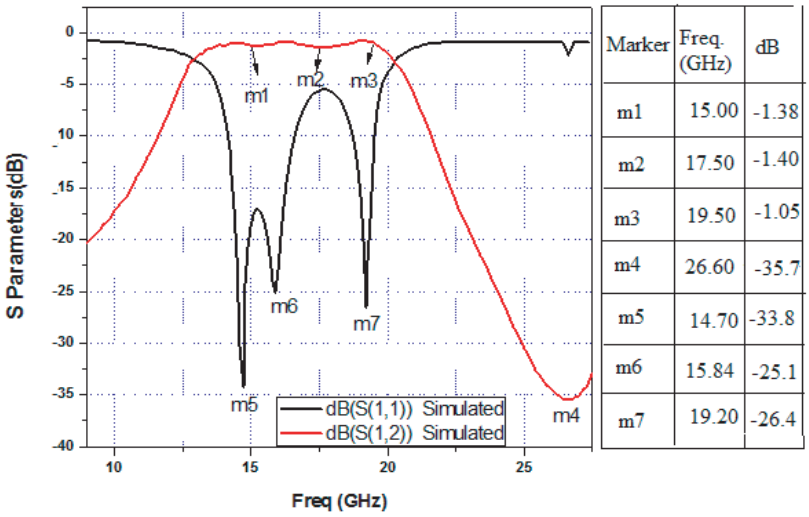

Marker	Freq. (GHz)	dB
m1	15.00	-1.38
m2	17.50	-1.40
m3	19.50	-1.05
m4	26.60	-35.7
m5	14.70	-33.8
m6	15.84	-25.1
m7	19.20	-26.4

Figure 9. Simulated response of C slot FSIW.

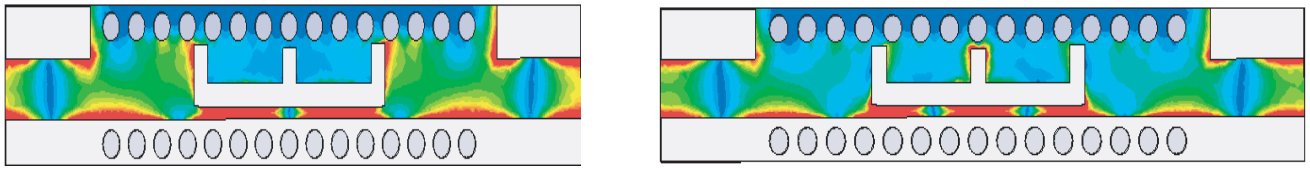

(a) (b)

Figure 10. Current distribution of E slot FSIW at (a) 14.7 GHz, (b) 19.2 GHz.

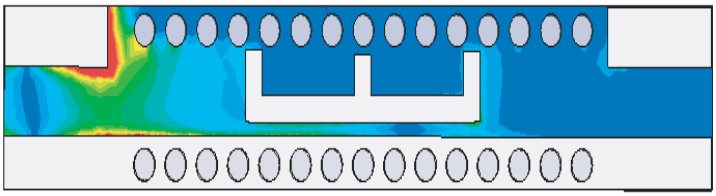

Figure 11. Current distribution of E slot FSIW in stop band.

at the peak resonance frequency of the first passband, current distribution is concentrated on side arms of E slot whereas at the resonant frequency of the second passband, the current distribution intensity is concentrated on the centre arm of E slot. From the current distribution it can be validated that the first passband is predominantly controlled by the side arms whereas the second passband is controlled by the centre arm of E slot which enhances its bandwidth approximately by 34.82%. This can be explained with the help of average current path length and its relationship with resonant frequency [15]. Fig. 11 shows the current distribution of E slot FSIW in stopband.

Further the first band's frequency shifts to lower side in E slot FSIW causing miniaturization in size as compared to C slot FSIW. This shift in frequency to lower side can be explained on basis of lumped equivalent circuit as shown in Fig. 12.

In this equivalent circuit, the presence of components L and C_{eq} are caused by the fractal slot etched on the central layer. The shunt capacitor C_C is created due to capacitive coupling between the two substrates of the folded waveguide, and inductance L_s is caused by the via. The slot loaded middle conducting plane can be taken as a parallel combination of equivalent capacitance and inductance. The

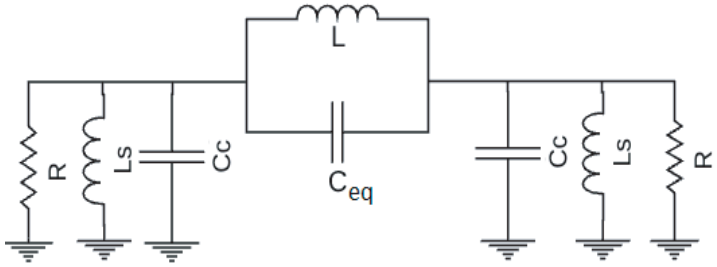

Figure 12. Equivalent lumped circuit of slotted FSIW filter.

total equivalent capacitance C_{eq} is due to the combination of coupling capacitance (due to the coupling of two substrate layers) along with slot capacitance [16]. The expression of the equivalent capacitance can be written as:

$$C_{eq} = C_1 + C_s \tag{8}$$

After slot loading, the new resonant frequency becomes:

$$f_0 = \frac{1}{2\pi\sqrt{LC_{eq}}} \tag{9}$$

The above equation justifies the gradual decrease of resonant frequency with the addition of slot as the capacitive reactance is increased by adding more slots.

5. FABRICATION AND RESULTS

To validate the result, the proposed filters are fabricated on substrate material glass PTFE with a relative dielectric constant of 2.5 and thickness of 1.6 mm for each layer using standard PCB process. Fig. 13(a) shows a photograph of the lower layer, and 13(b) shows a photograph of the top view of assembled filter with overall dimensions as: 27 mm (length including transition) × 11.5 mm (width) × 3.2 mm (height). The scattering parameters of the fabricated filter are measured by vector network analyzer HP 8510A. The measured and HFSS simulated results are compared and depicted in Fig. 14.

From Fig. 14, it is evident that measured bandwidth of the fabricated filter is from 15.75 GHz to 17.79 GHz with absolute bandwidth of 2.04 GHz (fractional bandwidth is approximately 20%). In the measured response of C slot FSIW, the maximum value of insertion loss is −1.40 dB with average value lying below −1.25 dB. Also in the passband, S_{11} has minimum values as −24.56 dB at 16.3 GHz and −21.2 dB at 17.20 GHz, respectively. There is a slight deviation in bandwidth and return loss in the measured result which may be attributed to the slight mismatch between feedline impedance and

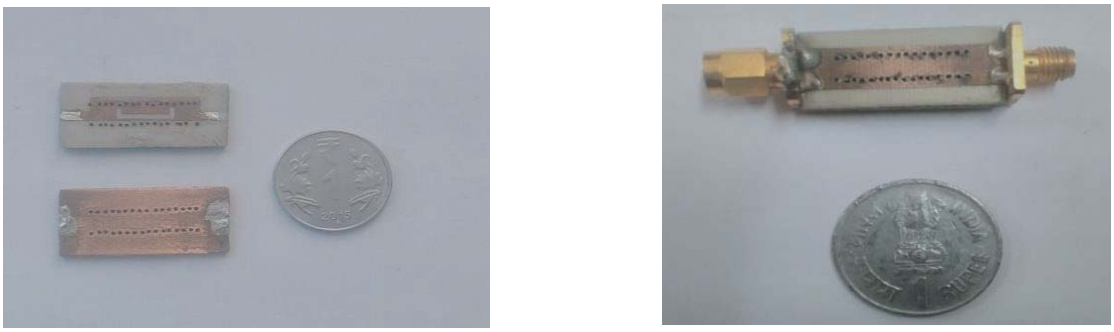

(a) (b)

Figure 13. (a) Top and bottom view of lower layer of C slot FSIW. (b) Top view of assembled filter.

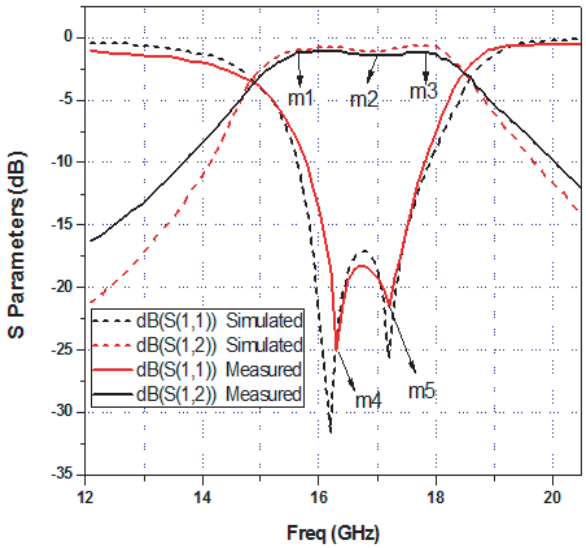

Marker	Freq. (GHz)	dB
m1	15.65	-1.25
m2	17.0	-1.40
m3	17.75	-1.17
m4	16.30	-24.56
m5	17.20	-21.20

Figure 14. Simulated and measured S-parameters of C slot FSIW.

(a) (b)

Figure 15. (a) Top and bottom view of lower layer of E slot FSIW. (b) Top view of assembled filter.

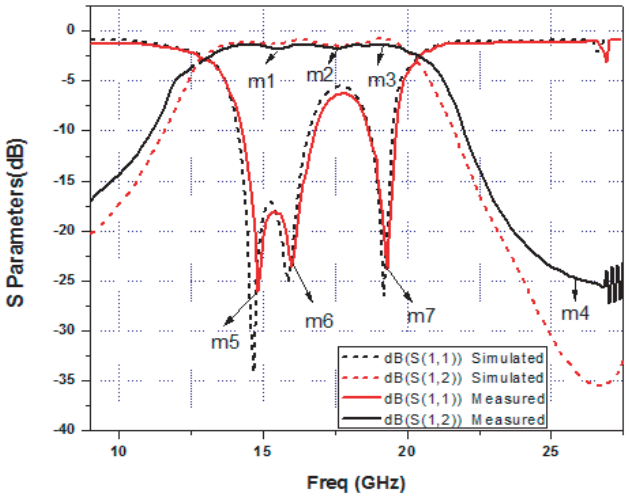

Marker	Freq. (GHz)	dB
m1	15.60	-1.78
m2	17.50	-1.74
m3	19.30	-1.42
m4	26.12	-24.8
m5	14.82	-25.92
m6	16.0	-23.40
m7	19.22	-23.80

Figure 16. Simulated and measured S-parameters of E slot FSIW.

connector's impedance caused by manual soldering of SMA connectors and misalignment of a few of vias during fabrication.

Figures 15(a) and (b) show photographs of the fabricated E slot FSIW filter layer wise and that of assembled filter, respectively. The measured and HFSS simulated results are compared and depicted in Fig. 16.

From Fig. 16, it is evident that measured bandwidth of the fabricated filter is from 14.35 GHz to 16.76 GHz with absolute bandwidth of 2.41 GHz in the first passband (fractional bandwidth of 15.58%) and from 18.66 GHz to 19.61 GHz with absolute bandwidth of 0.95 GHz in the second passband (fractional bandwidth of 5.30%). Also in the second passband, S_{11} has minimum value as 23.8 dB at 19.22 GHz. Hence the total bandwidth for E slot FSIW is found to be 3.35 GHz (fractional bandwidth of 20.8%). Further, the insertion loss over the passband is nearly -1.5 dB except a few points where it slightly goes below the value, but not less than -2 dB.

To illustrate the performance of the proposed filter, comparisons between the proposed filter and several previous SIW bandpass filters, reported in the references, are summarized in Table 1.

Table 1. Comparison of proposed filter with previous filters from reference.

Reference	Frequency band	Centre Frequency (GHz)	Return Loss (dB)	Insertion Loss (dB)	Fractional Bandwidth (%)
[17]	Ku	12.9/15.4	> 19	1	2.68
[18]	K	20.5	> 20	1.2	5.2
[19]	Ku	12.5	> 15	1.3	9
[20]	Ku & K	18.3	> 15	1.35	10.9
Proposed work	Ku & K	14.5/19.2	> 18	< 1.5	20.8

6. RESULTS AND CONCLUSION

In this paper, two folded SIW bandpass filter with different slot shapes (C and E shaped slot) are simulated and fabricated. The result shows that by introducing an additional slot, there is enhancement in the bandwidth. With C slot FSIW, there is only single passband of bandwidth 2.04 GHz and by introduction of slot at the centre of C slot to obtain E-slot FSIW, and the dual-band response in K/Ku band is achieved with significant enhancement in bandwidth by 67.5%. Further introduction of additional slot results in slight miniaturization of filter size by approximately 10%. Overall, there is good agreement between the simulated and measured results.

REFERENCES

1. Panagopoulos, A. D., S. Scalise, B. Ottersten, J. D. Kanellopoulos, and P. Burzigotti, "Special issue on satellite communication systems and networking," *EURASIP Journal of Wireless Communications and Networking*, Vol. 2012, 283, 2012.
2. De Sanctis, M., E. Cianca, G. Araniti, I. Bisio, and R. Prasad, "Satellite communications supporting internet of remote things," *IEEE Internet of Things Journal*, Vol. 3, No. 1, 113–122, Feb. 2016.
3. Deslandes, D. and K. Wu, "Single-substrate integration technique of planar circuits and waveguide filters," *IEEE Trans. Microw. Theory Tech.*, Vol. 51, No. 2, 593–596, 2003.
4. Bozzi, M., A. Georgiadis, and K. Wu, "Review of substrate-integrated waveguide circuits and antennas," *IET Microw. Antennas Propag.*, Vol. 5, No. 8, 909–920, 2011.
5. Chen, R. S., S.-W. Wong, and L. Zhu, "Wideband bandpass filter using U-slotted substrate integrated waveguide (SIW) cavities," *IEEE Microwave and Wireless Components Letters*, Vol. 25, No. 1, Jan. 2015.

6. Dong, K., J. Mo, Y. He, Z. Ma, and X. Yang, "Design of a millimetre-wave wideband bandpass filter with novel slotted substrate integrated waveguide," *Microwave and Optical Technology Letters*, Vol. 58, No. 10, 2406–2410, 2016.
7. Hosseini-Fahraji, A., K. Mohammadpour-Aghdam, and R. Faraji-Dana, "Design of wideband millimeter-wave bandpass filter using substrate integrated waveguide," *IEEE Iranian Conference on Electrical Engineering (ICEE)*, Shiraz, Iran, May 2016.
8. Liu, C. and X. An, "A SIW-DGS wideband bandpass filter with a sharp roll-off at upper stopband," *Microwave and Optical Technology Letters*, Vol. 59, No. 4, 789–792, Apr. 2017.
9. Wu, Y.-D., G.-H. Li, W. Yang, and X. Yang, "Design of compact wideband QMSIW band-pass filter with improved stopband," *Progress In Electromagnetics Research Letters*, Vol. 65, 75–79, 2017.
10. Che, W., L. Geng, K. Deng, and Y. L. Chow, "Analysis and experiments of compact folded substrate-integrated waveguide," *IEEE Trans. Microw. Theory Tech.*, Vol. 56, No. 1, 88–93, Jan. 2008.
11. Grigoropoulos, N., B. S. Izquierdo, and P. R. Young, "Substrate integrated folded waveguides (SIFW) and filters," *IEEE Microwave and Wireless Components Letters*, Vol. 15, No. 12, 829–831, Dec. 2005.
12. Muchhal, N. and S. Srivastava, "Review of recent trends on miniaturization of substrate integrated waveguide (SIW) components," *3rd IEEE International Conference on Computational Intelligence & Communication Technology (CICT)*, ABES Ghaziabad, India, Feb. 2017.
13. Kordiboroujeni, Z. and J. Bornemann, "Designing the width of substrate integrated waveguide structures," *IEEE Microwave and Wireless Components Letters*, Vol. 23, No. 10, 518–522, Oct. 2003.
14. User Manual Ansys Inc., "High Frequency Structural Simulator (HFSS) Software," ver.13.
15. Hu, H.-T., F.-C. Chen, and Q.-X. Chu, "A wideband U-shaped slot antenna and its application in MIMO terminals," *IEEE Antennas and Wireless Propagation Letters*, Vol. 15, 508–511, 2016.
16. Shivnarayan, S. Sharma, and B. R. Vishwakarma, "Analysis of slot loaded microstrip patch antenna," *Indian Journal of Radio and Space Physics*, Vol. 34, 424–430, Dec. 2005.
17. Li, G.-H., X.-Q. Cheng, H. Jian, and H.-Y. Wang, "Novel high-selectivity dual-band substrate integrated waveguide filter with multi-transmission zeros," *Progress In Electromagnetics Research Letters*, Vol. 47, 7–12, 2014.
18. Chen, X.-P. and K. Wu, "Substrate integrated waveguide cross-coupled filter with negative coupling structure," *IEEE Trans. Microw. Theory Tech.*, Vol. 56, No. 1, 142–149, Jan. 2008.
19. Diedhiou, D. L., E. Rius, J.-F. Favennec, and A. El Mostrah, "Ku-band cross-coupled ceramic SIW filter using a novel electric cross-coupling," *IEEE Microwave and Wireless Components Letters*, Vol. 25, No. 2, 109–111, Feb. 2015.
20. Rhbanou, A., M. Sabbane, and S. Bri, "Design of K-band substrate integrated waveguide band-pass filter with high rejection," *Journal of Microwaves, Optoelectronics and Electromagnetic Applications*, Vol. 14, No. 2, 155–169, 2015.